

Kinetics of Simultaneous Transformations

H. K. D. H. Bhadeshia

Department of Materials Science and Metallurgy, University of Cambridge, U.K.

Keywords: Avrami, overall transformation kinetics, simultaneous transformations, impingement

Abstract

It is quite frequent for a number of solid–state transformations to occur concurrently, starting from the same parent phase. The transformations may occur at different rates, but the resulting competition for space or for the partitioning of driving force between the precipitating phases can be seminal to the development of many microstructures found in commercial alloys. This paper reviews the overall transformation theory available for dealing with simultaneous transformations. The theory discussed is generally applicable, but is illustrated with specific reference to secondary hardening steels and structural steels.

Introduction

There are at least three circumstances in which a phase might transform into more than one product:

1. The equilibrium precipitate may be difficult to nucleate. Consequently, decomposition starts with the formation of one or more metastable phases which are kinetically favoured. These must eventually dissolve as equilibrium is approached. There are classic examples of this in the age–hardening of aluminium alloys and in secondary hardening steels. A recent example is the crystallisation of metallic glass, at first to a metastable phase [1]. In each case, the formation of the metastable phase is accompanied by a reduction in free energy causing an exaggerated retardation of the stable phase.
2. All of the product phases may be at equilibrium; *e.g.* the transformation of austenite into a mixture of ferrite and graphite. However, the transformation products do not grow in a coupled manner and may be sufficiently separated in time to be treated as *sequential* rather than *simultaneous*.
3. The product phases may be coupled as in the formation of pearlite, with a common transformation front.

It is the first case which forms the subject of this review.

Avrami Theory

A model for a single transformation begins with the calculation of the nucleation and growth rates using classical theory, but an estimation of the volume fraction requires impingement between particles to be taken into account. This is generally done using the extended volume concept of Johnson, Mehl, Avrami, and Kolmogorov [*e.g.* 2] as illustrated in Fig. 1 (henceforth referred to as “Avrami theory”). Suppose that two particles exist at time t ; a small interval δt later, new regions marked a , b , c & d are formed assuming that they are able to grow unrestricted in extended space whether or not the region into which they grow is already transformed. However, only those components of a , b , c & d which lie in previously untransformed matrix can contribute to a change in the real volume of the product phase (identified by the subscript ‘1’) :

$$dV_1 = \left(1 - \frac{V_1}{V}\right)dV_1^e \quad (1)$$

where it is assumed that the microstructure develops randomly. The superscript e refers to extended volume, V_1 is the volume of 1 and V is the total volume. Multiplying the change in extended volume by the probability of finding untransformed regions has the effect of excluding regions such as b , which clearly cannot contribute to the real change in volume of the product. For a random distribution of precipitated particles, this equation can easily be integrated to obtain the real volume fraction,

$$\frac{V_1}{V} = 1 - \exp\left\{-\frac{V_1^e}{V}\right\} \quad (2)$$

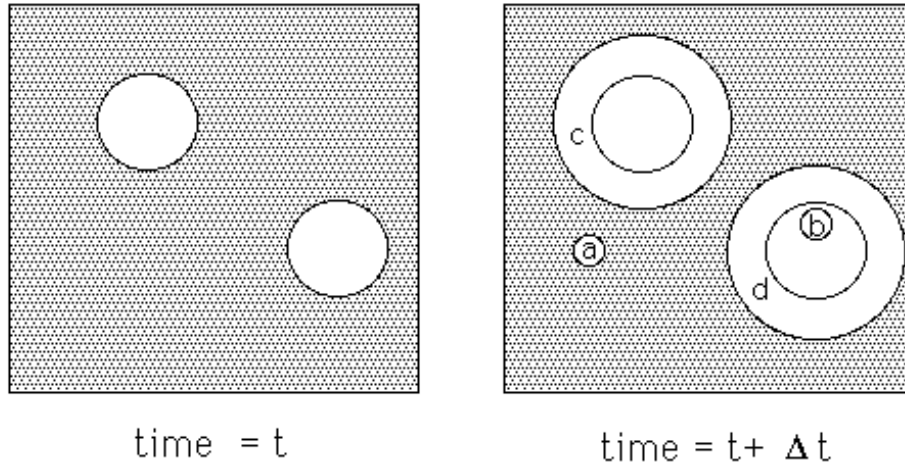


Fig. 1: An illustration of the concept of extended volume. Two precipitate particles have nucleated together and grown to a finite size in the time t . New regions c and d are formed as the original particles grow, but a & b are new particles, of which b has formed in a region which is already transformed.

Simultaneous Transformations

A simple modification for two precipitates (1 and 2) is that the equation 2 becomes a coupled set of two equations,

$$dV_1 = \left(1 - \frac{V_1 + V_2}{V}\right) dV_1^e \quad \text{and} \quad dV_2 = \left(1 - \frac{V_1 + V_2}{V}\right) dV_2^e \quad (3)$$

The method can be used for any number of reactions happening together. The resulting set of equations must in general must be solved numerically although a few analytical solutions are possible for special cases which we shall now illustrate.

Special Cases

For the simultaneous formation of two phases whose extended volumes are related linearly [3,4,5]:

$$V_2^e = BV_1^e + C \quad \text{with} \quad B \geq 0 \quad \text{and} \quad C \geq 0 \quad (4)$$

then with $v_i = V_i/V$, it can be shown [5] that

$$v_1 = \int \exp\left\{-\frac{(1+B)V_1^e + C}{V}\right\} \frac{dV_1^e}{V} \quad \text{and} \quad v_2 = Bv_1 \quad (5)$$

If the isotropic growth rate of phase 1 is G and if all particles of phase 1 start growth at time $t = 0$ from a fixed number of sites N_V per unit volume then $V_1^e = N_V \frac{4\pi}{3} G^3 t^3$. We emphasize that the specific assumptions made to express V_1^e can be selected at will, for example to include a nucleation rate (details can be found in Christian [2]). On substitution of the extended volume in equation 5 gives

$$v_1 = \frac{1}{1+B} \exp\left\{-\frac{C}{V}\right\} \left[1 - \exp\left\{-\frac{(1+B)N_V \frac{4\pi}{3} G^3 t^3}{V}\right\}\right] \quad \text{with} \quad v_2 = Bv_1 \quad (6)$$

The term $\exp\{-C/V\}$ is the fraction of parent phase available for transformation at $t = 0$; it arises because $1 - \exp\{-C/V\}$ of phase 2 exists prior to commencement of the simultaneous reaction at $t = 0$. Thus, v_2 is the additional fraction of phase 2 that forms during simultaneous reaction. When $C = 0$, equations 6 reduce to the case considered by Robson and Bhadeshia [3]. It is emphasized that $C \geq 0$. A case for which $C = 0$ and $B = 8$ is illustrated in Fig. 2.

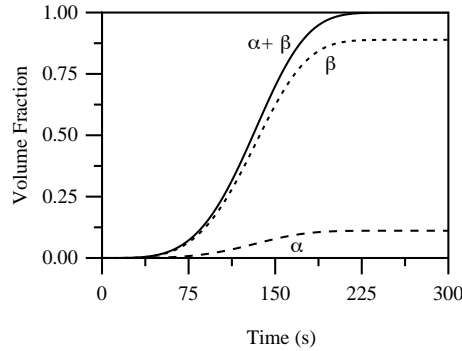


Fig. 2: Simultaneous transformation to phases $\alpha \equiv 1$ and $\beta \equiv 2$ with $C = 0$ and $B = 8$.

For the case where the extended volumes are related parabolically [5]:

$$v_1 = \exp\left\{-\frac{C}{V}\right\} \left[\sqrt{\frac{\pi}{4A}} \exp\left\{\frac{(1+B)^2}{4A}\right\} \left(\operatorname{erf}\left\{\frac{1+B}{\sqrt{4A}} + \sqrt{AV_1^e}\right\} - \operatorname{erf}\left\{\frac{1+B}{\sqrt{4A}}}\right\} \right) \right] \quad (7)$$

$$v_2 = \exp\left\{-\frac{C}{V}\right\} \left[1 - \exp\left\{-\frac{A(V_1^e)^2 + (1+B)V_1^e}{V}\right\} \right] - v_1$$

The volume fractions v_i again refer to the phases that form *simultaneously* and hence there is a scaling factor $\exp\{-C/V\}$ which is the fraction of parent phase available for coupled transformation to phases 1 and 2.

Secondary Hardening Steels

Whereas the analytical cases are revealing, it is unlikely in practice for the phases to be related in the way described. This is illustrated for secondary hardening steels of the kind used commonly in the construction of power plant [3]. The phases interfere with each other not only by reducing the volume available for transformation, but also by removing solute from the matrix and thereby changing its composition. This change in matrix composition affects the growth and nucleation rates of the phases.

The calculations must allow for the simultaneous precipitation of M_2X , $M_{23}C_6$, M_7C_3 , M_6C and Laves phase. M_3C is assumed to nucleate instantaneously with the paraequilibrium composition. Subsequent enrichment of M_3C as it approaches its equilibrium composition is accounted for. All the phases, except M_3C , are assumed to form with compositions close to equilibrium

[3]. The driving forces and compositions of the precipitating phases are calculated using standard thermodynamic methods.

The interaction between the precipitating phases is accounted for by considering the change in the average solute level in the matrix as each phase forms. This is frequently called the “mean field approximation”. It is necessary because the locations of precipitates are not predetermined in the calculations.

A plot showing the predicted variation of volume fraction of each precipitate as a function of time at 600 °C is shown in Fig. 3. It is worth emphasising that there is no prior knowledge of the actual sequence of precipitation, since all phases are assumed to form at the same time, albeit with different precipitation kinetics. The fitting parameters common to all the steels are the site densities and interfacial energy terms for each phase [3]. The illustrated dissolution of metastable precipitates is a natural consequence of changes in the matrix chemical composition as the equilibrium state is approached.

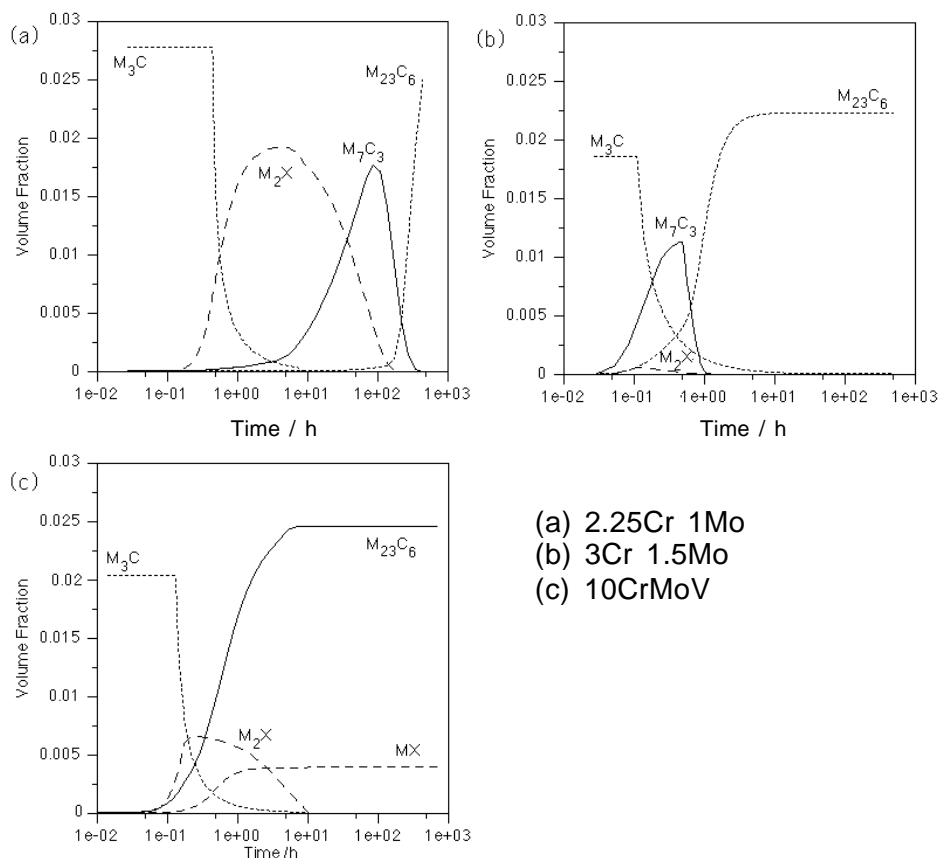


Fig. 3: The predicted evolution of precipitate volume fractions at 600 °C for three power plant materials (a) Fe-0.15C-2.12Cr-0.9Mo-0.5Mn-0.17Ni wt%; (b) Fe-0.1C-3Cr-1.5Mo-1Mn-0.1Ni-0.1V and (c) Fe-0.11C-10.22Cr-1.42Mo-0.5Mn-0.55Ni-0.12V-0.5Nb-0.056N (after [3]).

Consistent with experiments, the precipitation kinetics of $M_{23}C_6$ are predicted to be much slower in the 2.25Cr1Mo steel compared to the 10CrMoV and 3Cr1.5Mo alloys. One contributing factor is that in the 2.25Cr1Mo steel a relatively large volume fraction of M_2X and M_7C_3 form prior to $M_{23}C_6$. These deplete the matrix and therefore suppress $M_{23}C_6$ precipitation. The volume fraction of M_2X which forms in the 10CrMoV steel is relatively small, and there remains a considerable excess of solute in the matrix, allowing $M_{23}C_6$ to precipitate rapidly. Similarly,

in the 3Cr1.5Mo steel the volume fractions of M_2X and M_7C_3 are insufficient to suppress $M_{23}C_6$ precipitation to the same extent as in the 2.25Cr1Mo steel.

It is even possible in this scheme to treat precipitates nucleated at grain boundaries separately from those nucleated at dislocations, by taking them to be different phases in the sense that the activation energies for nucleation will be different.

The computer program for doing these calculations is available freely on the world wide web [6]. We note for the moment, that this is as far as microstructure modelling has progressed. Work is in progress to calculate size distributions by avoiding the conversion from extended to real volume. This is reasonable when the volume fractions of precipitate phases are small because the probability of particle impingement can be negligible.

Ferrite, Widmanstätten ferrite and Pearlite

There have been many studies about the occurrence of Widmanstätten ferrite in steels as a function of the chemical composition, austenite grain size and the cooling rate during continuous cooling transformation. It is understood that Widmanstätten ferrite is favoured in austenite with a large grain structure. This is probably because Widmanstätten ferrite is rarely found in isolation but often forms as secondary plates growing from allotriomorphic ferrite layers. The prior formation of allotriomorphic ferrite, which is favoured by a *small* grain size, enriches the residual austenite with carbon, so it is not surprising that a small austenite grain size suppresses Widmanstätten ferrite. For the same reason, an increase in cooling rate will tend to favour the formation of Widmanstätten ferrite.

These and other concepts are implicitly built into the model based on simultaneous transformation kinetics [3–5]. This is because allotriomorphic ferrite, Widmanstätten ferrite and pearlite are allowed to grow together assuming that thermodynamic and kinetic conditions are satisfied. Their interactions are all taken into account during the course of transformation.

The reasonable overall level of agreement between experiment and theory is illustrated in Fig. 4, for data from [7]. In all cases where the allotriomorphic ferrite content is underestimated, the Widmanstätten ferrite content is overestimated. This is expected both because the composition of the austenite changes when allotriomorphic ferrite forms and because its formation changes the amount of austenite that is free to transform to Widmanstätten ferrite.

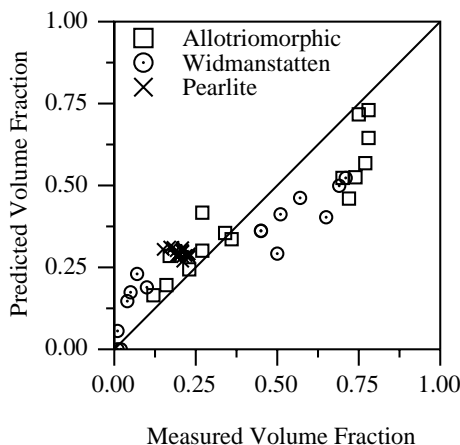


Fig. 4: A comparison of the calculated volume fraction versus experimental data reported by Bodnar and Hansen [7].

Fig. 5 shows calculations which illustrate how the model can be used to study the evolution of microstructure as the sample cools [4]. The computer program for these calculations can be obtained freely from the world wide web [6].

All of the generally recognised trends are reproduced. The amount of Widmanstätten ferrite clearly increases with the austenite grain size, and with the cooling rate within the range considered. Bodnar and Hansen [7] suggested also that the effect of cooling rate on the amount of Widmanstätten ferrite was smaller than that of the austenite grain size (for the values considered). This is also evident in Fig. 5.

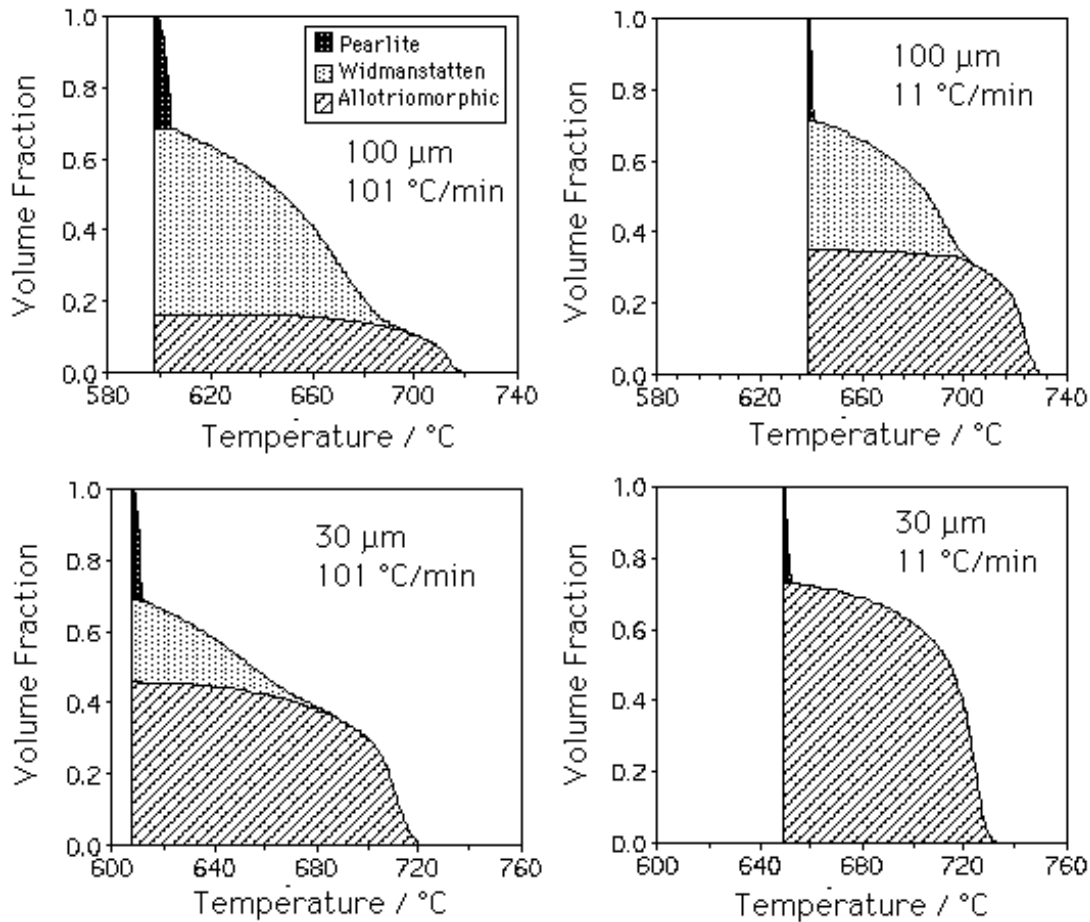


Fig. 5: Calculated evolution of microstructure in a sample of Fe-0.18C-0.48Si-1.15Mn as a function of the austenite grain size and the cooling rate [4].

The work has been applied to the competition of allotriomorphic and idiomorphic ferrite as a function of the number densities of austenite grain surface and intragranular nucleation sites [8]. One result is illustrated in Fig. 6 for a particular steel *c* [8]. A reduction in the austenite grain size should lead to a change in the balance between allotriomorphic and idiomorphic ferrite. Data are presented for austenite grain sizes of 150, 50 and 25 μm . The reduction in the austenite grain size leads to a change from an idiomorphic to allotriomorphic ferrite dominated transformation. Such an effect is well established from a qualitative point of view; large austenite grain sizes favour intragranularly nucleated transformation products for two reasons. Firstly, the number density of grain boundary nucleation sites decreases relative to intragranular sites as d_γ is increased. Secondly, grain boundary nucleation sites are generally more potent than inclusions so transformation commences first at the boundaries. Therefore, assuming a constant thickness of allotriomorphic ferrite along the austenite grain boundaries, a reduction in the austenite grain size leads to a larger volume fraction of allotriomorphic ferrite.

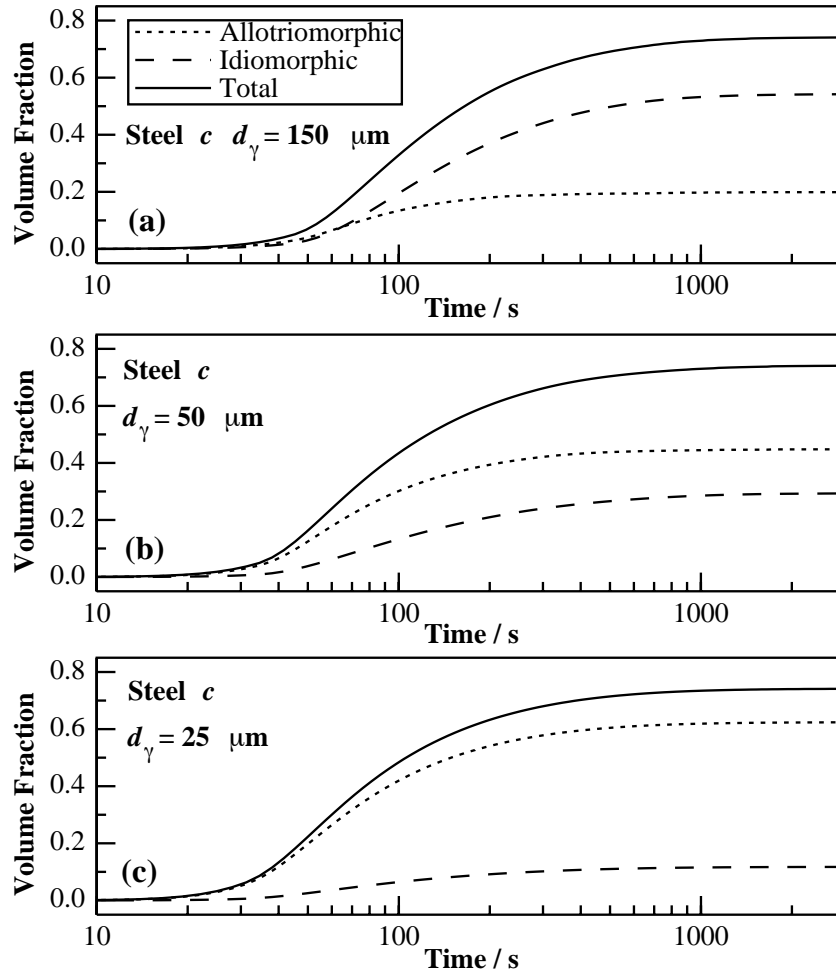


Fig. 6: Transformations in a particular steel *c* described in reference [8]. (a) An austenite grain size of $150 \mu m$; (b) an austenite grain size of $50 \mu m$; (c) an austenite grain size of $25 \mu m$.

Applications of the theory of simultaneous transformations have also been made to the estimation of microstructure in steel weld deposits [9].

Deconvolution of Simultaneous Transformations

The tempering of martensite in steels occurs by the formation of metastable carbides before the precipitation of cementite is completed. The tempering process is often followed indirectly by monitoring the change in electrical resistivity, thermoelectric power or hardness. These parameters, when normalised with respect to zero time and infinite time define an overall “fraction” which is taken to represent the entire set of reactions involved on the atomic scale.

The variation of fraction with time is frequently found to deviate from a simple sigmoidal relationship, presumably because the curve actually represents more than one reaction occurring at the same time. There have been a number of attempts to deconvolute such master curves into components due to individual reactions.

Hanawa and Mimura [10], following work by Yamamoto [11], defined relaxation times (τ) which are related empirically to the formation or dissolution of phases during simultaneous transformation:

$$\frac{dy}{dt} = -\left(\frac{1}{\tau_1} + \frac{1}{\tau_2}\right)y + \frac{y_1}{\tau_3}$$

where y has a value of unity when none of the excess solute is precipitated, and zero when all of the excess is precipitated. y_1 and y_2 represent the fractions of metastable and stable precipitates respectively, such that $1 - y = y_1 + y_2$. τ_1 , and τ_2 are the relaxations times for the precipitation of the metastable and stable phases respectively, and τ_3 the corresponding term for the dissolution of the metastable phase. The relaxation times are inversely proportional to the reaction rate constant. With boundary conditions and certain other modifications, these equations can be fitted to experimental data to deconvolute the overall y versus time t curve.

Luiggi and Betancourt [12–14] have followed a similar phenomenological approach which appears mathematically to be general in form, although it too requires a large number of fitting parameters.

Although attempts have been made in all of these cases to deduce parameters such as activation energies, it is difficult to see whether these are physically meaningful. For example, because each reaction involves nucleation and growth, there should be more than one thermally activated process for each phase.

Summary

There has been some progress in the theory for the overall transformation kinetics simultaneous transformations. In particular, the Johnson–Mehl–Avrami–Kolmogorov concept of extended volume can be adapted for the case where more than one reaction occurs at the same time. It is suggested that further effort should focus on the treatment of: (a) the consequences, if any, of the mean field approximation of the impingement of solute diffusion fields; (b) a more rigorous treatment of multicomponent effects; (c) the incorporation of coarsening as a natural phenomenon within the overall model.

Acknowledgments

I am grateful to Professor Alan Windle for the provision of laboratory facilities at the University of Cambridge, to the organisers of PTM '99 for inviting me to present this work, and to Joe Robson, Stephen Jones, Kazutoshi Ichikawa, Nobuhiro Fujita and Tadashi Kasuya for valuable discussions on the subject of simultaneous transformations over the course of many years.

References

- 1) J. Y. Bang and R. Y. Lee: *Journal of Materials Science*, **26** (1991) 4961–4965.
- 2) J. W. Christian: *Theory of Transformations in Metals and Alloys*, Part 1, 2nd edition, Pergamon Press, Oxford (1975)
- 3) J. Robson and H. K. D. H. Bhadeshia: *Materials Science and Technology* **13** (1997) 631–639.
- 4) S. Jones and H. K. D. H. Bhadeshia: *Acta Materialia* **45** (1997) 2911–2920.
- 5) T. Kasuya, K. Ichikawa, M. Fuji and H. K. D. H. Bhadeshia: *Materials Science and Technology*, (1999) in press.
- 6) Materials Algorithms Project, MAP: Perpetual Library of Computer Programs, (1999) [www.msm.cam.ac.uk /map/mapmain.html](http://www.msm.cam.ac.uk/map/mapmain.html)
- 7) R. L. Bodnar and S. S. Hansen: *Metallurgical and Materials Transactions A*, **25A** (1994) 763–773
- 8) S. Jones and H. K. D. H. Bhadeshia: *Metallurgical and Materials Transactions A*, **28A** (1997) 2005–2013.
- 9) K. Ichikawa and H. K. D. H. Bhadeshia: *Mathematical Modelling of Weld Phenomena 3*, eds. H. Cerjak and H. K. D. H. Bhadeshia, Institute of Materials, London, (1997) 181–198.
- 10) K. Hanawa and T. Mimura: *Metallurgical Transactions A* **15A** (1984) 1147–1153.
- 11) S. Yamamoto: *Trial of New Rate Theory* (in Japanese), Showado, Kyoto, referred to by Hanawa and Mimura (1979) 178–196.
- 12) N. J. Luiggi and A. Betancourt: *Metallurgical and Materials Transactions B*, **25B** (1994) 917–925.

- 13) N. J. Luigi and A Betancourt: Metallurgical and Materials Transactions B, **25B** (1994) 927–935.
- 14) N. J. Luigi and A Betancourt: Metallurgical and Materials Transactions B, **25B** (1997) 161–168.

To appear in *Proceedings of Solid-Solid Phase Transformations '99*, published by the Japan Institute of Materials, 1999.